Cystine Peptides: The Intramolecular Antiparallel β-Sheet Conformation of a 20-Membered Cyclic Peptide Disulfide

R. KISHORE, *Molecular Biophysics Unit, Indian Institute of Science;* S. RAGHOTHAMA, *Sophisticated Instruments Facility, Indian Institute of Science;* and P. BALARAM,* *Molecular Biophysics Unit, Indian Institute of Science, Bangalore 560 012, India*

Synopsis

A 20-membered cyclic peptide disulfide

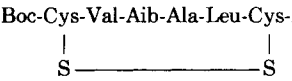

has been synthesized as a conformational model for disulfide loops of limited ring size. ^{1}H-nmr studies at 270 MHz establish the presence of three intramolecular hydrogen bonds involving the Leu, Val, and methylamide NH groups in $CDCl_3$. Evidence for peptide aggregation in $CDCl_3$ is also presented. A structural transition involving loosening of the hydrogen bond formed by the Val NH group is observed upon the measured addition of $(CD_3)_2SO$ to $CDCl_3$. Hydrogen-bonding studies, together with unusually low field positions of the Cys(1) and Cys(6) $C^{\alpha}H$ resonances and high $J_{HNC^{\alpha}H}$ values provide support for an intramolecular antiparallel β-sheet conformation, facilitated by a chain reversal at the Aib-Ala segment. Extensive nuclear Overhauser effect studies provide compelling evidence for the proposed conformation and also establish a type I′ β-turn at the Aib-Ala residues, the site of the chain reversal.

INTRODUCTION

Small disulfide loops containing a limited number of intervening amino acids between the two linked cysteine residues

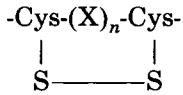

form an important structural element in proteins and polypeptide hormones. We have undertaken a systematic investigation of the conformational properties of small disulfide loops varying in size from 11- (one spacer residue) to 20- (four spacer residues) membered rings. Earlier reports from this laboratory described the conformational analysis of 14-membered cyclic peptide disulfides,[1-4] which assume importance in view of their occurrence at the active

* To whom correspondence should be addressed.

Biopolymers, Vol. 26, 873–891 (1987)

CCC 0006-3525/87/060873-19$04.00

site of redox proteins, like thioredoxin and glutaredoxin.[5,6] Our interest in cystine peptides has also been stimulated by the possibility of using disulfide cross-links to stabilize specific peptide conformations.[7-9] In this report we present a detailed study of the solution conformation of a 20-membered cyclic peptide disulfide

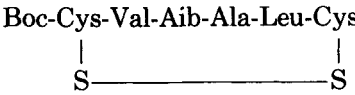

(1)*

(all chiral amino acids are of the L-configurations) which can serve as a model for an antiparallel β-sheet conformation bridged by an S-S linkage. The choice of amino acid sequence was dictated by the following requirements: good solubility in apolar organic solvents, where intramolecular hydrogen-bonded conformations would be stabilized; convenient, unequivocal assignment of the ^{1}H-nmr spectrum; the central location of the Aib-Ala segment, chosen to facilitate β-turn formation[10-15] in view of the well-known propensity of Aib-X sequences to adopt such reverse-turn conformations[12-15]; terminal blocking groups to provide additional CO and NH groups for intramolecular hydrogen bonding. Thus, such a peptide may provide a model for systems like glutathione reductase,[16] lipoamide dehydrogenase,[17] and mercuric reductase,[18] where the 20-membered active-site disulfide loop is flanked by other residues. It is noteworthy that in the best-studied 20-membered disulfide loops like oxytocin, vasopressin, and their analogs,[19,20] one of the Cys residues is at the amino terminus and pH-dependent structural transitions have been observed.[21] Furthermore, Cys(6), in the neurohypophyseal hormones, is followed by a proline residue, which lacks an NH group for intramolecular hydrogen bonding. Thus, the neutral sequence chosen in this study may be useful in evaluating structural possibilities for such loops in proteins. The results described in this report establish an *intramolecular* antiparallel β-sheet conformation, nucleated by a chain reversal involving an Aib-L-Ala β-turn.

EXPERIMENTAL

Synthesis and Characterization of Peptides

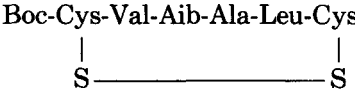

(1)

was synthesized by conventional solution-phase procedures following the strategy outlined in Scheme 1. Detailed procedures are essentially similar to those described for tetrapeptide disulfides.[1,4] The intermediate peptides were fully characterized by ^{1}H-nmr (60 and 270 MHz) and checked for purity by thin layer chromatography (TLC) (silica gel) in the following solvent systems: A = 5% MeOH–$CHCl_3$, B = *n*-butanol–acetic acid–H_2O (4 : 1 : 1). The acyclic,

*Boc, tert-butyloxycarbonyl; Bzl, benzyl; NHMe, N-methylamide DCC, N,N′-dicyclohexyl carbodiimide; DMF, N,N-dimethylformamide; HOBt, 1-hydroxybenzotriazole.

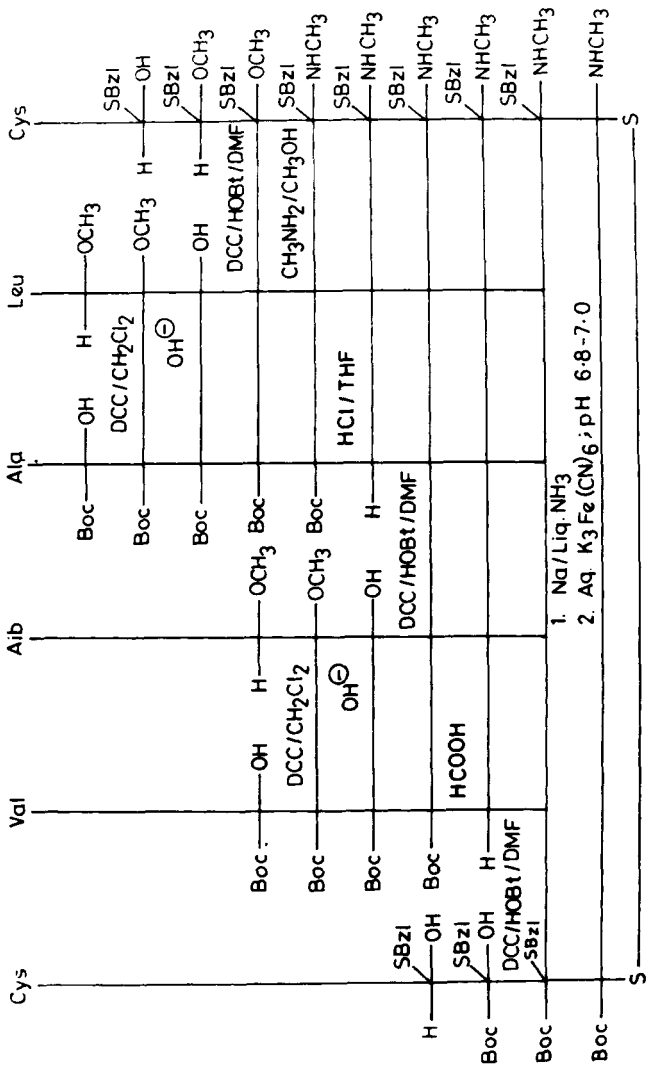
Cys
Val
Aib
Ala
Leu
Cys
Boc
H
OH
SBzl
OCH3
NHCH3
DCC/CH2Cl2
OH⊖
DCC/HOBt/DMF
CH3NH2/CH3OH
HCl/THF
HCOOH
1. Na/Liq. NH3
2. Aq. K3Fe(CN)6; pH 6·8-7·0
S

Scheme 1.

protected precursor, Boc-Cys(SBzl)-Val-Aib-Ala-Leu-Cys(SBzl)-NHMe, was also purified by silica gel column chromatography. The physical characteristics [mp (°C), $[\alpha]_D^{25}$ (c = 0.3, MeOH), R_f(A)] of key intermediates are listed below: Boc-Ala-Leu-Cys(SBzl)-OMe, 96°, −87°, 0.83; Boc-Ala-Leu-Cys(SBzl)-NHMe, 128°, −70°, 0.49; H-Ala-Leu-Cys(SBzl)-NHMe, 107°, −40°, 0.19; Boc-Val-Aib-Ala-Leu-Cys(SBzl)-NHMe, 170°, −50°, 0.23; H-Val-Aib-Ala-Leu-Cys(SBzl)-NHMe, 155°, −53°, 0.21; Boc-Cys(SBzl)-Val-Aib-Ala-Leu-Cys(SBzl)-NHMe, 150°, −55°, 0.32.

Reductive cleavage of the benzyl groups of the acyclic hexapeptide, Boc-Cys(SBzl)-Val-Aib-Ala-Leu-Cys(SBzl)-NHMe, (1.8 g, 2 mmol) by Na/liquid NH_3 and subsequent oxidative cyclization in aqueous solution (1500 mL) by $K_3Fe(CN)_6$ (0.02*M*, pH 6.8–7.0), was carried out as described earlier.[1-4] The crude product was purified over a silica gel column, using $CHCl_3$ and $CHCl_3$-MeOH mixtures for elution. The most intense component (I_2 visualization) on silica gel TLC of the crude product was isolated as a white crystalline solid and shown to be the hexapeptide disulfide **1**. Yield: 0.23 g (27%); mp = 180°C; $[\alpha]_D^{25}$ (c = 0.3, MeOH) = −63°C; R_f(A) = 0.17. The peptide was shown to be homogeneous by high performance liquid chromatography on a Lichrosorb RP-18 column (linear gradient elution, 60–85% MeOH–H_2O in 25 min, flow rate 0.8 mL min^{-1}, detection 226 nm, retention time 19.1 min). A fast atom bombardment mass spectrum of **1** yielded an MH^+ peak at 704, confirming the monomeric structure (M_r = 703). The peptide was fully characterized by its 270 MHz ^{1}H-nmr (Fig. 1) and 67.89 MHz ^{13}C-nmr spectra (data not shown).[22]

Spectroscopic Studies

Nuclear magnetic resonance studies were carried out on a Bruker WH-270 FT nmr spectrometer equipped with an Aspect 2000 computer at the Sophisticated Instruments Facility, Indian Institute of Science, as described earlier.[7,23] All chemical shifts are expressed as δ (ppm) downfield from internal $(Me)_4Si$. In the difference nuclear Overhauser effect (NOE) experiments, the perturbed and normal spectra recorded sequentially (one on-resonance and one off-resonance) in different parts of the memory (8 K each), were obtained by low power on-resonance saturation of a peak and by off-resonance shifting of the irradiation frequency, respectively. About 100 transients were accumulated with an acquisition time of 1.368 s and a relaxation delay of 3 s. The FIDs were multiplied by an exponentially decaying function before Fourier transformation and the difference is taken on the transformed spectra. Undegassed samples were used in the NOE experiments. A peptide concentration of ~ 30 m*M* was used in the NOE studies to obtain good signal-to-noise ratios, while a concentration of ~ 14 m*M* was employed for other nmr studies.

Two-dimensional correlated spectroscopy (COSY) spectra[24,25] were recorded using a spectral width of 3012 Hz in both F_1 and F_2 dimensions. The number of data points were 256 in F_1 and 512 in F_2. The data were multiplied with a phase-shifted sine bell before Fourier transformation. Zero filling was applied in the F_1 dimension only. The total acquisition time was 2 h.

Infrared spectra were recorded in dilute $CHCl_3$ solutions on a Perkin-Elmer Model 297 spectrometer using a pathlength of 4 mm.

RESULTS AND DISCUSSION

A fully assigned 270-MHz ^{1}H-nmr spectrum of **1** in $CDCl_3$ is shown in Fig. 1. The urethane NH [Cys(1)] was assigned by virtue of its high field position in $CDCl_3$.[1-4,23] The methylamide and Aib NH groups were readily recognized by their appearance as a quartet and singlet, respectively. The assignment of the spin systems corresponding to the remaining residues was made by COSY[24,25] (Fig. 2). Conventional spin decoupling experiments carried out in the early part of these studies were also used for confirmation. The overlap and complexity of the Leu $C^{\gamma}H$ and $C^{\beta}H_2$ resonances renders tracing of this spin system ambiguous.[26] However, the presence of only a single Leu residue in **1** prevents any ambiguity in assignments. The corresponding assignments in $(CD_3)_2SO$ were obtained by monitoring spectral changes in $CDCl_3$–$(CD_3)_2SO$ mixtures of varying composition. The relevant parameters for the NH and $C^{\alpha}H$ groups in **1** are summarized in Table I. The extremely large spread of NH chemical shifts (~ 5.50–8.50 ppm), the high $J_{HNC^{\alpha}H}$ values (> 8.5 Hz) for all residues, except Ala and the extraordinarily low-field resonance positions for the Cys(1) and Cys(6) $C^{\alpha}H$ resonances, indicate a well-defined folded conformation for **1** in $CDCl_3$.

Delineation of Hydrogen-Bonded NH Groups

The presence of solvent-shielded or intramolecularly hydrogen-bonded NH groups was established using the following criteria[27-29]: (a) temperature dependence of NH chemical shifts in $CDCl_3$ and $(CD_3)_2SO$, (b) paramagnetic radical induced line broadening, (c) solvent dependence of NH chemical shifts in $CDCl_3$–$(CD_3)_2SO$ mixtures and rates of hydrogen–deuterium exchange in $(CD_3)_2SO$–D_2O mixtures.

Studies in $CDCl_3$

The temperature dependence of NH chemical shifts in $CDCl_3$ was found to be linear over the range 294–324 K, and the temperature coefficient ($d\delta/dT$) values of the NH resonances are listed in Table I. In $CDCl_3$, the Ala NH exhibits a very low $d\delta/dT$ value (0.0009 ppm/K), while the Aib NH exhibits a very high $d\delta/dT$ value (0.01 ppm/K). Of the remaining five NH groups, Cys(1), Cys(6), and methylamide have relatively high $d\delta/dT$ values (0.005–0.007 ppm/K), while Val and Leu have moderate temperature coefficients (0.003–0.004 ppm/K). In an apolar, poor hydrogen bond accepting solvent like $CDCl_3$, both solvent-shielded and solvent-exposed NH groups can give rise to low temperature coefficients. The NH groups involved in intermolecular hydrogen bonds are characterized by high $d\delta/dT$ values, due to breakage of the intermolecular interactions at elevated temperatures.[30-32] Alternatively, high $d\delta/dT$ values in $CDCl_3$ may also be indicative of weak intramolecular hydrogen bonds, which are broken on heating.[30-32]

In order to evaluate the possibility of peptide aggregation in $CDCl_3$, the concentration dependence of peptide NH chemical shifts for **1** in $CDCl_3$ was determined. Studies have been carried out over the concentration range of 0.57–47 mM, and results are summarized in Fig. 3. Three NH groups—Aib, Cys(6), and Cys(1)—move downfield with increasing concentration, indicating

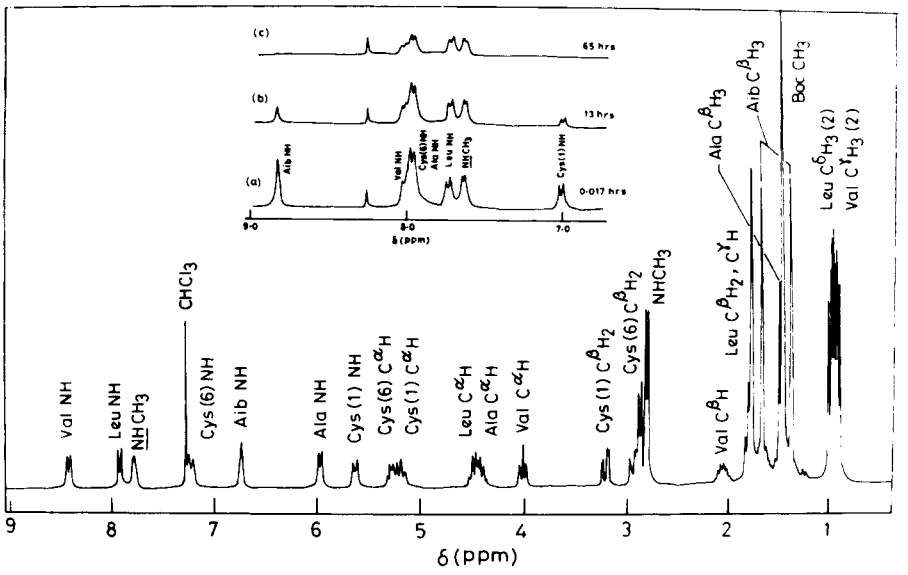

Fig. 1. 270-MHz ^{1}H-nmr spectrum of

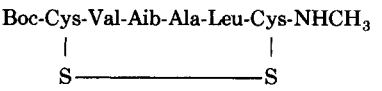

in $CDCl_3$. (Inset) Peptide NH resonances in $(CD_3)_2SO$ as a function of time after addition of D_2O (10%).

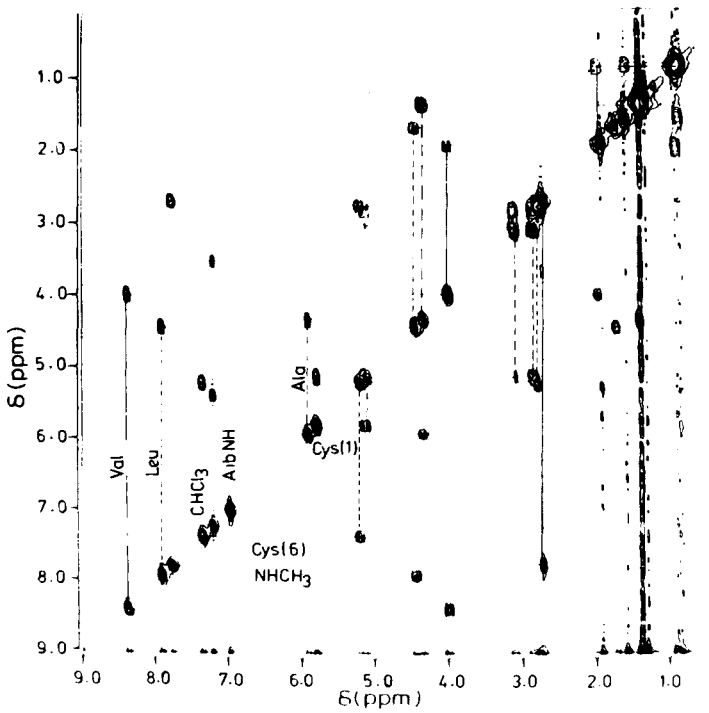

Fig. 2. COSY spectrum of 1 indicating connectivity of resonances corresponding to individual residues.

TABLE I

270-MHz ^{1}H-nmr Parameters[a] for Boc-Cys-Val-Aib-Ala-Leu-Cys-$NHCH_3$

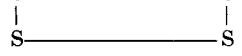

Parameters	Residue						
	Cys(1)	Val	Aib	Ala	Leu	Cys(6)	$\underline{NH}CH_3$
δ_{NH} ($CDCl_3$)[a]	5.63	8.41	6.72	5.97	7.92	7.23	7.79
δ_{NH} ($(CD_3)_2SO$[a]	7.01	8.07	8.79	7.92	7.67	7.89	7.64
$^3J_{HNC^{\alpha}H}$ ($CDCl_3$)[b]	10.2	9.4	—	7.6	8.6	10.0	—
$^3J_{HNC^{\alpha}H}$ ($(CD_3)_2SO$[b]	8.6	6.4	—	5.3	7.6	5.3	—
$\delta_{C^{\alpha}H}$ ($CDCl_3$)[a]	5.17	4.00	—	4.41	4.49	5.27	—
$\delta_{C^{\alpha}H}$ ($(CD_3)_2SO$[a]	4.35	3.98	—	3.94	4.27	4.52	—
$d\delta/dT$ ($CDCl_3$)[c]	0.0051	0.0030	0.0107	0.0009	0.0042	0.0072	0.0058
$d\delta/dT$ ($(CD_3)_2SO$[c]	0.0065	0.0058	0.0044	0.0045	0.0006	0.0031	0.0034

[a] δ values are expressed as ppm downfield from internal TMS and reported for a peptide concentration of ~ 14 mM in both $CDCl_3$ and $(CD_3)_2SO$.

[b] Errors in J values are ± 0.4 Hz.

[c] $d\delta/dT$ values are expressed as ppm/K measured at a concentration of ~ 14 mM in both $CDCl_3$ and $(CD_3)_2SO$.

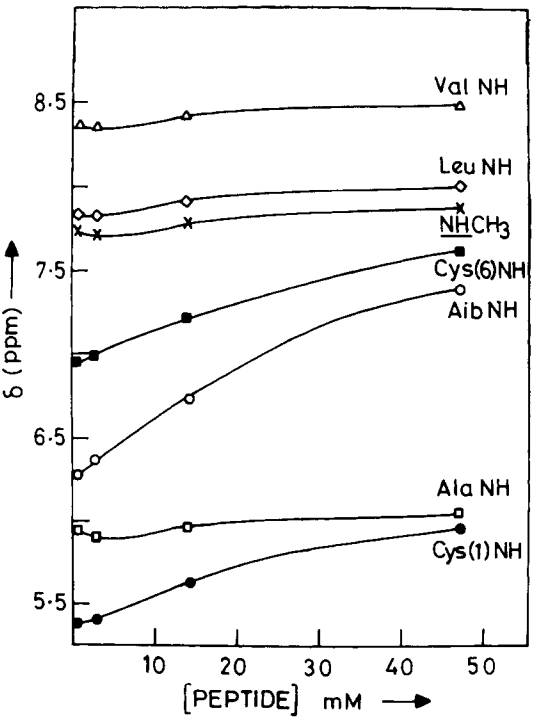

Fig. 3. Concentration dependence of NH chemical shifts in $CDCl_3$ for peptide **1**.

that these NH groups participate in the formation of intermolecular hydrogen bonds. On the other hand, the Val, Leu, methylamide, and Ala NH groups show very little concentration dependence. Thus, these four NH groups may participate in either *intramolecular* interactions or remain as solvent-exposed NH groups even at high peptide concentration. Figure 4 shows the effect of

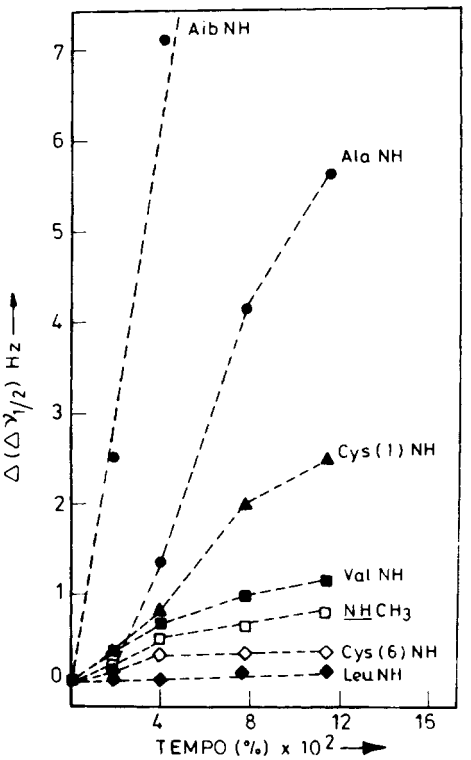

Fig. 4. Effect of the free radical TEMPO on the linewidths of peptide NH resonances in $CDCl_3$. $\Delta(\Delta\nu_{1/2})$ is the line broadening in the presence of TEMPO.

the addition of the paramagnetic radical TEMPO on the NH resonances of **1**. The extent of line broadening follows the order Aib NH ≫ Ala NH > Cys(1) NH > Val NH ≈ methylamide NH ≈ Cys(6) NH ≈ Leu NH. Extensive line broadening is seen for the Aib and Ala NH groups, whereas the Cys(1) NH is relatively less affected. The remaining four NH groups [Val, Cys(6), Leu, and methylamide] are inaccessible to the radical. It is interesting to note that the Ala NH group exhibits significant line broadening in this experiment, suggesting its exposure to the solvent in $CDCl_3$.

The results of the radical perturbation experiment together with temperature and concentration dependence of NH chemical shifts lead to the following conclusions:

1. The Ala and Aib NH groups are solvent exposed at low peptide concentration. At high peptide concentration the Aib NH participates in *intermolecular* hydrogen bonds, whereas the Ala NH remains exposed to solvent.

2. The Cys(1) NH group is solvent exposed but participates in intermolecular association at high peptide concentration. The Val, methylamide, and Leu NH groups are shielded from the solvent, and do not participate in intermolecular association. However, the moderate $d\delta/dT$ value obtained in $CDCl_3$ for these three NH groups suggests that they may be involved in intramolecular interactions, which are weakened at higher temperatures.

3. The Cys(6) NH participates in intermolecular association, but appears relatively shielded even at low peptide concentration, as compared to the other NH groups [Cys(1), Ala, and Aib].

Studies in $(CD_3)_2SO$

The plots of NH chemical shifts vs temperature were found to be linear over the temperature range of 293–253 K. The $d\delta/dT$ values are summarized in Table I. The $d\delta/dT$ values of NH resonances in $(CD_3)_2SO$ clearly suggest that the Leu, methylamide, and Cys(6) NH groups (< 0.004 ppm/K) are solvent shielded, whereas the Aib, Cys(1), Val, and Ala NH groups (> 0.004 ppm/K) are exposed to the bulk solvent. It is interesting to note that the Leu NH exhibits an extremely low $d\delta/dT$ value (0.0006 ppm/K), suggesting that this NH group is strongly solvent shielded in $(CD_3)_2SO$.

A hydrogen–deuterium (H-D) exchange experiment carried out for peptide **1** in a $(CD_3)_2SO$–D_2O mixture is illustrated in the inset to Fig. 1. The results of this experiment clearly indicate that the Cys(1) and Aib NH groups are solvent exposed in $(CD_3)_2SO$, whereas the Leu and methylamide NH groups are solvent shielded. In Fig. 1, note (inset) that the Val, Cys(6), and Ala NH groups overlap and form a composite peak in the nmr spectrum after addition of D_2O to a $(CD_3)_2SO$ solution. However, careful inspection of these peaks reveals that one of the NH resonances exchanges relatively slowly, as compared to the other two NH resonances. This resonance may be assigned to the Cys(6) NH group, since this proton exhibits a relatively low $d\delta/dT$ value (0.0031 ppm/K) in $(CD_3)_2SO$, in contrast to the Ala and Val NH groups, which exhibit high $d\delta/dT$ values in $(CD_3)_2SO$ (see Table I). Thus the H-D exchange experiment provides clear evidence for the solvent-shielded nature of the Leu and methylamide NH groups in $(CD_3)_2SO$. The Cys(6) NH group also appears partially shielded from the solvent.

Studies in $CDCl_3$–$(CD_3)_2SO$ Mixtures

The addition of a strong hydrogen-bonding solvent like $(CD_3)_2SO$ to a peptide solution in a poorly hydrogen-accepting solvent like $CDCl_3$ can result in large perturbations of the chemical shifts of solvent-exposed NH groups. A study of the nmr spectra in $CDCl_3$–$(CD_3)_2SO$ mixtures can also be useful in monitoring conformational transitions, which may take place with a change in solvent polarity.

The solvent dependence of NH and $C^{\alpha}H$ chemical shifts in $CDCl_3$–$(CD_3)_2SO$ mixtures are illustrated in Figs. 5 and 6. The Ala, Aib, and Cys(1) NH groups exhibit large downfield shifts with increasing $(CD_3)_2SO$ concentration, confirming their exposure to the solvent, while the Cys(6) NH group is relatively less affected. The methylamide, Leu, and Val NH groups exhibit anomalous solvent-titration curves, with the unusual effects most pronounced for the Val NH resonance. The Leu NH shows an initial *downfield* shift on addition of $(CD_3)_2SO$, followed by a moderate *upfield* shift at higher $(CD_3)_2SO$ concentration. This may imply that, at higher $(CD_3)_2SO$ concentrations, the Leu NH is relatively less accessible to solvent. This is further reflected in a very low $d\delta/dT$ value (0.0006 ppm/K) of Leu NH in $(CD_3)_2SO$. However, the methylamide and Val NH groups show an initial upfield shift on addition of $(CD_3)_2SO$, followed by downfield shifts at higher $(CD_3)_2SO$ concentrations. This effect is much more pronounced for the Val NH group, compared to the methylamide NH group. It is noteworthy that such solvent titration curves have been reported for NH groups in the case of cyclic biscystine peptides.[33] A definitive explanation for such anomalous solvent-titration curves is not

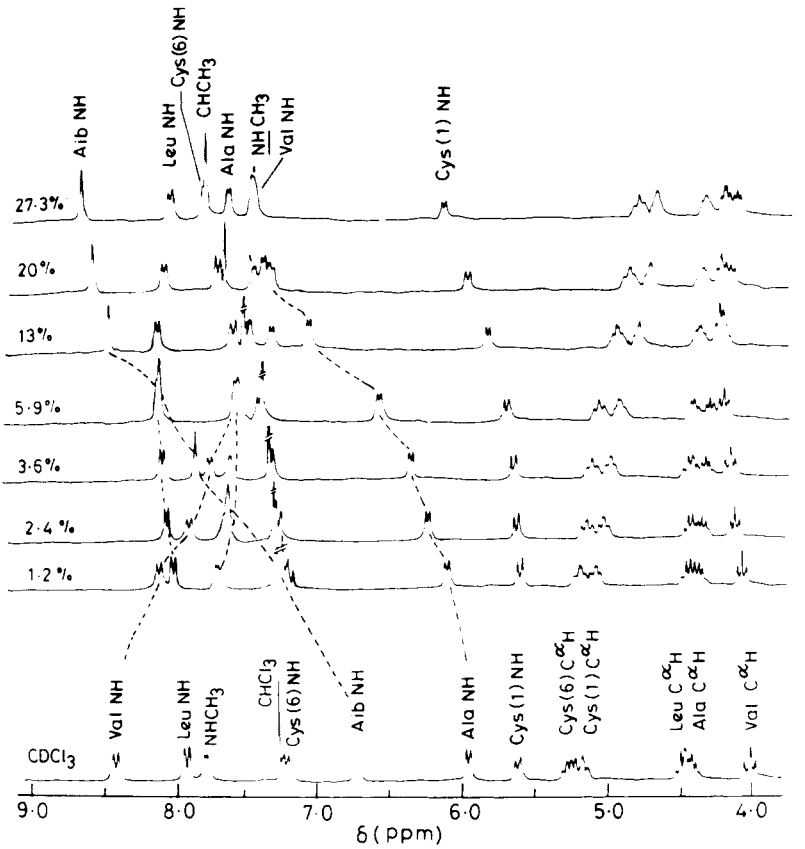

Fig. 5. Partial 270-MHz ^{1}H-nmr spectra of C$^\alpha$H and NH resonances in peptide 1 in $CDCl_3$–$(CD_3)_2SO$ mixtures of varying composition. $(CD_3)_2SO$ concentration (vol%) are indicated against the traces.

available at present. However, it is possible that at low concentrations of $(CD_3)_2SO$, peptide 1 may undergo a pronounced conformational change involving the Val residue, as shown from the sharp and rapid upfield shifts of Val NH in the initial stages of the titration. As a result of this conformational change, the Val NH becomes less accessible (shielded) to $(CD_3)_2SO$. However, at higher concentration of $(CD_3)_2SO$ ($\geq$ 12%), the Val NH exhibits a large downfield shift, characteristic of a solvent-exposed NH group. Thus, the solvent-titration experiment in $CDCl_3$–$(CD_3)_2SO$ mixtures provides evidence for a structural transition, which results in exposure of the Val NH group in $(CD_3)_2SO$. In conjunction with the studies described above in the pure solvent, the results establish that the Val NH is inaccessible to solvent in $CDCl_3$ but exposed in $(CD_3)_2SO$. Some evidence for a solvent-dependent conformational change is also seen from the altered chemical shifts of the Cys(1), Cys(6), and Val C$^\alpha$H protons in $(CD_3)_2SO$.

IR Studies

The NH- and CO-stretching bands in the ir spectra of peptide 1 in $CHCl_3$ as a function of peptide concentration are illustrated in Fig. 7. Bands due to

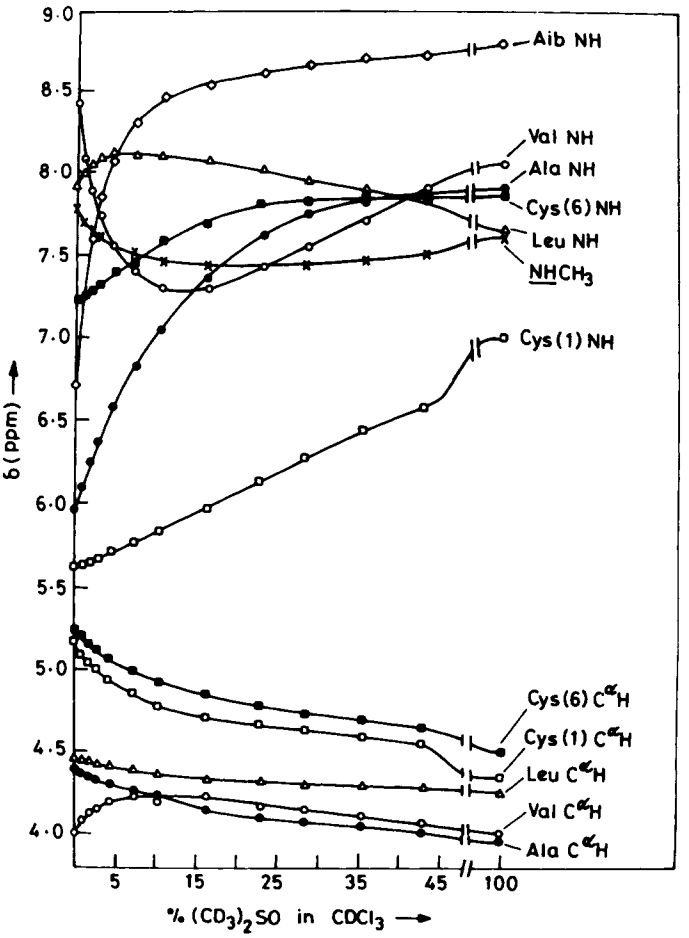

Fig. 6. Dependence of NH and $C^{\alpha}H$ chemical shifts in **1** as a function of solvent composition in $CDCl_3$–$(CD_3)_2SO$ mixtures.

both free NH [ν_{NH}(f)] and hydrogen-bonded NH [ν_{NH}(hb)] stretching vibrations are observed at ~ 3440 and ~ 3340 cm^{-1}, respectively.[34,35] The ir spectra also exhibit a distinctive shoulder at ~ 3470 cm^{-1}. The assignment of this band is not clear at present. However, it is certainly due to free NH group(s) in the molecule. The ν_{NH}(hb) band observed over the concentration range of 1.12–9.0 m*M* suggests that intramolecular hydrogen bonds contribute to this absorption band. The ν_{NH}(hb) is very broad (~ 3330–3370 cm^{-1}), suggesting that hydrogen bonds of different strengths may stabilize the solution conformation of peptide **1** in $CHCl_3$. The CO-stretching bands (amide I) are observed at ~ 1660 cm^{-1}. The ir spectra exhibit distinct shoulders at 1705 and 1650 cm^{-1}. The shoulder at 1705 cm^{-1} (urethane) is about 15–20 cm^{-1} lower than that observed in free urethane groups, suggesting involvement in hydrogen bonding.[33,35] The position of the amide I bands at 1660 and 1650 cm^{-1} (shoulder) is consistent with an antiparallel β-sheet conformation.[33,36]

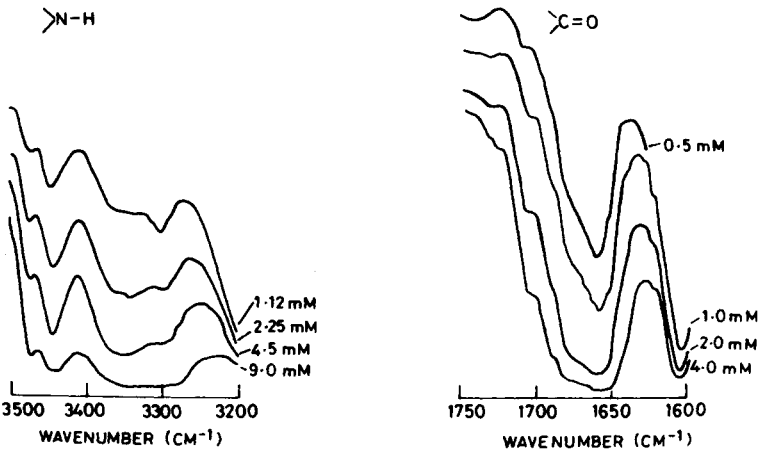

Fig. 7. Partial ir spectra of peptide 1 in $CHCl_3$ showing NH (left) and CO (right) stretching bands. Peptide concentrations are indicated against the traces.

Conformation of Peptide 1 Derived from Spectroscopic Data

The ir studies suggest that intramolecularly hydrogen-bonded conformations are populated for peptide 1 in $CHCl_3$. The nmr results in $CDCl_3$ provide strong support for the solvent-shielded nature of the Leu, Val, and methylamide NH groups. It is a reasonable inference that these three NH groups are involved in intramolecular hydrogen bonds. The nmr results also provide evidence for the steric shielding of the Cys(6) NH proton in $CDCl_3$.

A conformation consistent with the nmr data is shown in Fig. 8. The conformation involves three transannular, intramolecular hydrogen bonds formed between Val NH–Leu CO, Leu NH–Val CO, and methylamide NH–Boc CO groups. Thus, the molecule adopts an intramolecular, antiparallel β-sheet conformation generated by means of an Aib-Ala β-turn in the central part of the molecule. The unusual lowfield positions of the $C^{\alpha}H$ protons of Cys(1) and Cys(6) (5.17–5.27 δ), and NH protons of Val, Leu, and methylamide (the NH groups involved in intramolecular hydrogen bonds in $CDCl_3$) (7.79–8.41 δ) in $CDCl_3$, are presumably a consequence of such conformations.[33] Nuclear magnetic resonance studies of proteins suggest that relatively lowfield $C^{\alpha}H$ and NH resonances are characteristic of β-sheet conformations,[37,38] possibly as a consequence of short $C^{\alpha}H$-to-oxygen atom distances between nonneighboring residues in these structures.[39] The high vicinal coupling constant ($^3J_{HNC^{\alpha}H}$) values ($\geq$ 10 Hz) observed for Cys(1) and Cys(6) NH groups in $CDCl_3$, are consistent with an extended β-sheet conformation. The Leu and Val NH groups also exhibit large values of coupling constants (> 8.6 Hz). These values are compatible with $\phi \sim -130$ to $-140°$.[40]

Note that aggregation of peptide 1 in $CDCl_3$ can result from intermolecular hydrogen bonding involving the exposed NH and CO groups on the periphery of the molecule. The concentration dependence of NH chemical shifts in $CDCl_3$ suggests that Cys(1), Aib, and Cys(6) NH groups are indeed involved in such a process, supporting the formation of approximately planar, sheetlike structures at high peptide concentrations. It is significant that the central peptide unit of the β-turn, which lies approximately perpendicular to the

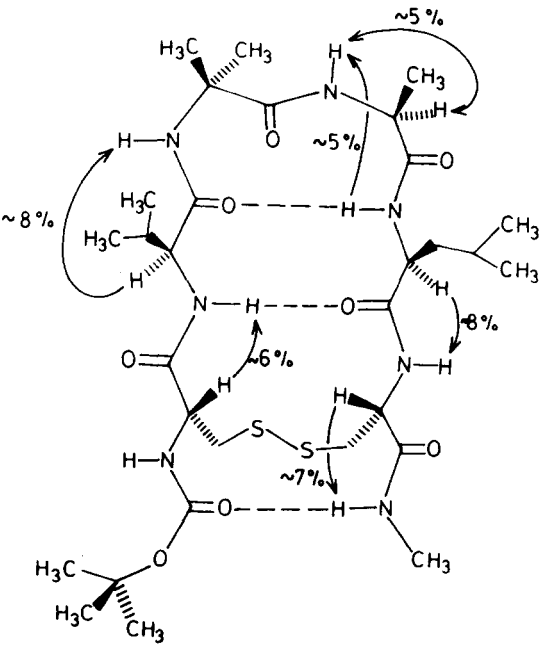

Fig. 8. Proposed antiparallel β-sheet conformation for peptide 1. Magnitude of key interresidue NOEs are indicated by arrows linking the two hydrogen atoms. Arrowhead indicates irradiated proton.

plane of the sheet, does not appear involved in an intermolecular interaction. This is evident from the lack of any concentration dependence for the nmr parameters of the Ala NH group.

In polar solvents like $(CD_3)_2SO$, peptide 1 can exist largely as solvated monomers. The nmr results provide evidence for subtle distortions in the conformation of peptide 1 on, going from an apolar solvent like $CDCl_3$ to a highly polar solvent like $(CD_3)_2SO$. For example, in Table I, the Cys(1) and Cys(6) $C^{\alpha}H$ protons move ~ 0.75 and 0.82 ppm upfield in $(CD_3)_2SO$ from the positions observed in $CDCl_3$. Further, the $^3J_{HNC^{\alpha}H}$ values for Cys(1), Cys(6), Leu, and Val in $(CD_3)_2SO$ are significantly lower than the values observed in $CDCl_3$. In $(CD_3)_2SO$, the Val NH is substantially exposed to the solvent, suggesting a weakening of the Val NH–Leu CO hydrogen bond. It appears that in $(CD_3)_2SO$ the Val CO–Leu NH, and the Boc CO–methylamide NH hydrogen bonds are retained, and Cys(6) NH is appreciably shielded from the solvent. A careful examination of the conformation proposed in Fig. 8 reveals that an ideal β-sheet structure results in a fairly close approach of the Val CO and Leu CO groups. This should, in principle, result in electrostatic destabilization due to unfavorable dipole–dipole interactions. Such an unfavorable interaction could be offset by strong linear CO–NH hydrogen-bond formation. In apolar solvents like $CDCl_3$, the formation of such transannular hydrogen bonds may be the conformational determinant. However, in a solvent like $(CD_3)_2SO$, the NH groups can form strong hydrogen bonds to solvent. In such a case, conformational changes involving rotation about Val ϕ,ψ and Leu ϕ,ψ

can result in destabilization of the Val NH–Leu CO hydrogen bond, while at the same time relieving the unfavorable Val CO and Leu CO interaction.

The β-turn hydrogen bond between Val CO and Leu NH groups is fairly strong, as evidenced from the very low $d\delta/dT$ value of the Leu NH in $(CD_3)_2SO$. This is undoubtedly due to the strong tendency of the Aib-Ala sequence to favor β-turn conformations. Extensive studies on Aib-containing peptides have established that this residue favors conformations having $\phi \sim \pm 60 \pm 20°$ and $\psi \sim \pm 30 \pm 20°$.[12-15] Since the conformation proposed in Fig. 8 requires that the Aib residue occupy the $i + 1$ position of the β-turn, it is necessary that only types I(III) or I′(III′) β-turns[10,11] be considered. A type II(II′) would require conformational angles of $\phi \sim -60°$ (60°), $\psi \sim 120°$ (−120°) for the Aib residue. Crystallographic studies of a large number of Aib peptides have so far failed to yield a single example of such a conformation for an Aib residue located centrally in an oligopeptide.[13-15] It is interesting to note that a shallow energy minimum is indeed observed for the Aib residue in this region of ϕ,ψ space, which is, however, significantly less favorable than the energy minimum in the region of $3_{10}/\alpha$-helical conformations.[13] An examination of molecular models reveals no evident steric strain in the 20-membered disulfide ring, thus suggesting that cyclization constraints may not be significant enough to force the lone Aib residue into an intrinsically less favorable conformation. The NOE data discussed below further excludes the type II (II′) β-turn structure.

NOE Studies

In order to further clarify the nature of the conformation adopted by **1** in organic solvents, NOE studies[7] have been carried out in $CDCl_3$, a 10% $(CD_3)_2SO$–$CDCl_3$ mixture, and $(CD_3)_2SO$.

Representative difference NOE spectra obtained by irradiation of NH resonances are shown in Figs. 9 and 10. The results of NOE studies are summarized in Table II. In $CDCl_3$ and 10% $(CD_3)_2SO$–$CDCl_3$ mixtures, the observed NOEs are positive, suggesting that rotational correlation times are short enough to be in the region $\omega\tau_c \ll 1$ at 270 MHz.[41,42] In $(CD_3)_2SO$, no appreciable NOEs were observed at the probe temperature of 293 K. On increasing the temperature to 318 K, weak positive NOEs could be detected (Fig. 10). These results suggest that in the highly viscous solvent, $(CD_3)_2SO$, peptide τ_c values are long enough to result in nonobservable NOEs. This observation once again emphasizes the difficulties encountered in NOE studies of oligopeptides, where unfavorable correlation times can result in lack of observed NOEs.[33,43,44]

Four *interresidue* NOEs ($C_i^\alpha H$–$N_{i+1}H$) are clearly observed. These are the Cys(1) $C^\alpha H \leftrightarrow$ Val NH, Val $C^\alpha H \leftrightarrow$ Aib NH, Leu $C^\alpha H \leftrightarrow$ Cys(6) NH, and Cys(6) $C^\alpha H \leftrightarrow$ methylamide NH (Fig. 9). In all cases, the magnitude of the NOE observed on the $C^\alpha H$ proton when the corresponding NH is irradiated is ~ 6–9% (Table II). The magnitudes of the observed NOEs in the reverse experiment, i.e., when the $C^\alpha H$ proton is irradiated and the NH proton is observed, are slightly smaller. This is consistent with the existence of alternative relaxation pathways for the NH protons. Small intraresidue effects between NH and $C^\alpha H$ protons of the same residue are sometimes observed.

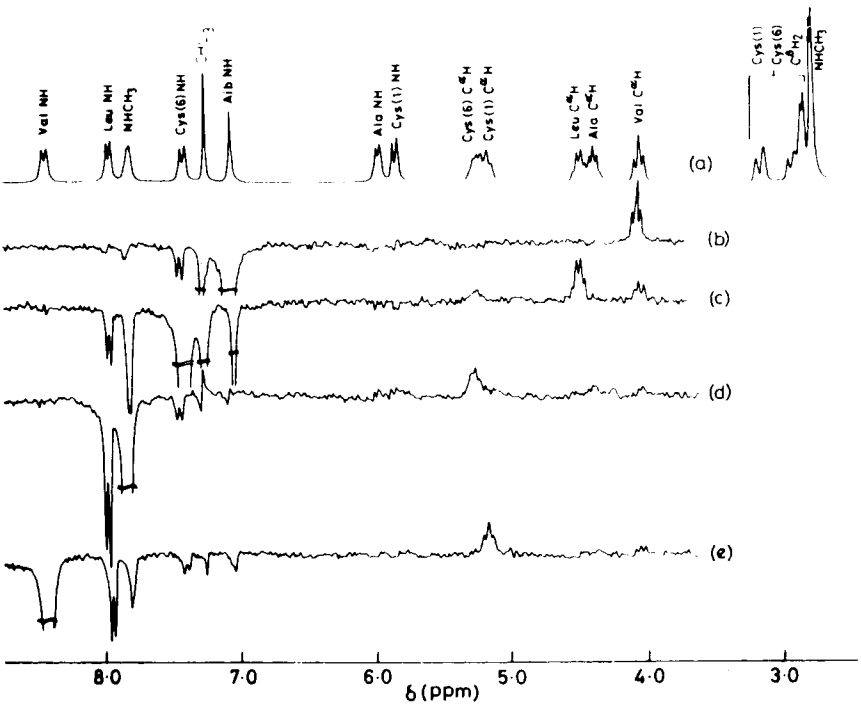

Fig. 9. (a) Partial 270-MHz ^{1}H-nmr spectrum of **1** in $CDCl_3$. (b–e) Difference NOE spectra (×16) obtained by saturation of specific NH resonances: (b) Aib NH, (c) Cys(6) NH, (d) methylamide NH, and (e) Val NH. The saturated peak appears as an intense negative signal in the difference spectrum.

A significant NOE of ~ 5.1% is observed on the Leu NH proton when Ala NH is saturated. Several NOEs are also observed on the saturation of the CH_3 groups of the Aib and Ala residues (Table II). All the observed NOEs in $CDCl_3$ are fully consistent with the antiparallel β-sheet conformation depicted in Fig. 8. In such a conformation, the Cys(1), Val, Cys(6), and Leu residues adopt structures having $\phi \sim -130° \pm 10°$, $\psi \sim +130° \pm 10°$, resulting in close approach (2.1–2.4 Å) of the $C_i^\alpha H$ and $N_{i+1}H$ protons.[45,46] In the Aib-Ala segment, the observation of the NOE between the Ala NH and Leu NH is a clear indicator of the β-turn conformation. An interproton distance of ~ 2.4 Å is expected between the $N_{i+2}H$ and $N_{i+3}H$ protons in both type I and type II β-turns.[45] Irradiation of the lowfield CH_3 proton of Aib (~ 1.67 δ) results in an 11% enhancement of the Ala NH proton. A substantial NOE of 5.3% is also observed between the Ala NH and Ala $C^\alpha H$ protons. However, no NOE is observed on the Ala NH proton when the Ala CH_3 resonance was saturated. From an examination of the model of peptide **1**, it is clear that these results favor $\phi \sim +90°$ for the Ala residue. ϕ values in this region lead to short interproton distance (< 2.5 Å) for the $C_i^\alpha H$ and N_iH protons.[46] The results support a type I′ β-turn conformation for the Aib-Ala segment (ideal Type I′ β-turn conformational angles are $\phi_{Aib} = +60°$, $\psi_{Aib} = +30°$; $\phi_{Ala} = +90°$, $\psi_{Ala} = 0°$).[5] This is somewhat unusual since L-Ala may have been expected to adopt negative ϕ values. However, there are precedents for the L-Ala residue adopting positive ϕ values in small peptides. For example, in the

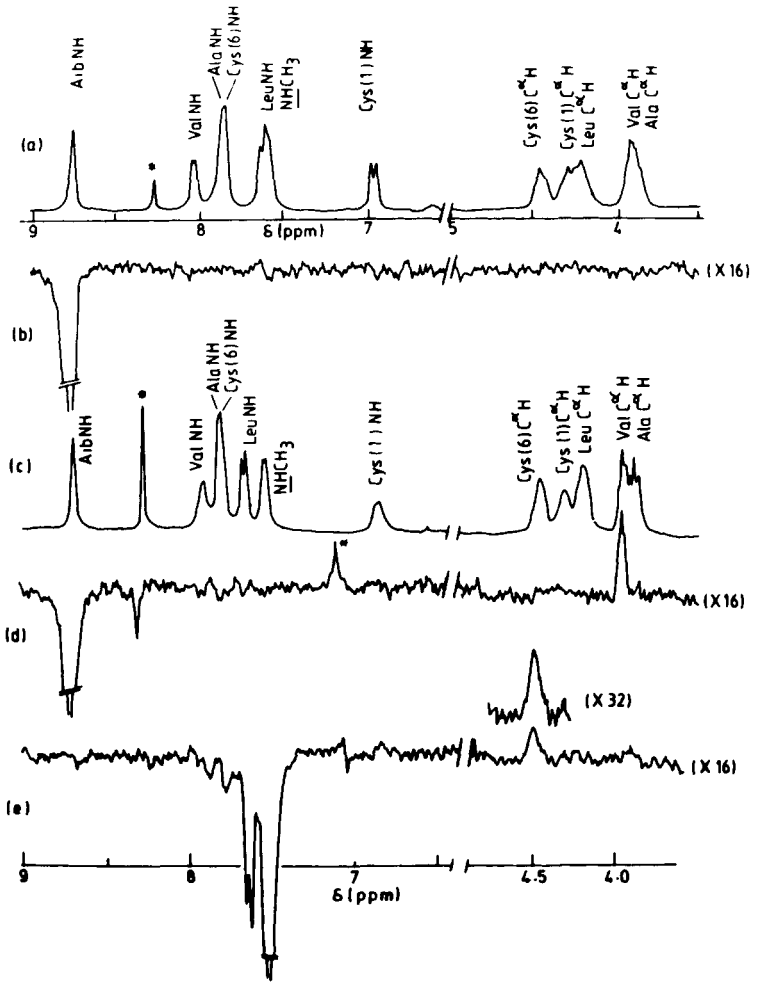

Fig. 10. Partial 270-MHz ^{1}-nmr spectra of **1** in $(CD_3)_2SO$ at (a) 293 K and (c) 318 K. (b, d, e) Difference NOE spectra obtained by irradiation of NH resonances: (b) Aib NH at 293 K, (d) Aib NH at 318 K, and (e) methylamide NH at 318 K. Resonance marked by an asterisk in a and c corresponds to $CHCl_3$ present in the sample. In d, an asterisk marks a spurious signal.

crystal structure of N-isobutyl-L-Pro-L-Ala-isopropylamide, the L-Ala residue adopts conformational angles $\phi = 66°$, $\psi = 14°$.[47] The NOE results presented earlier permit a definitive distinction between type I′ and type II′ β-turn conformations at the Aib-Ala segment. For a type I′ conformation structure, the Ala NH is expected to yield NOE connectivities to the Ala $C^{\alpha}H$ and one of the Aib methyl groups (*Pro-R* CH_3). In the type II′ structure, the Ala NH is expected to yield NOEs to the Ala CH_3 and the other Aib methyl group (*pro*-S CH_3). The experimental observations (Table II) clearly favor the type I′ structure.

The results presented in this report provide strong evidence in favor of an intramolecular antiparallel β-sheet conformation in peptide **1**. This study demonstrates the utility of cyclic peptide disulfides in generating relatively rigid models for specific peptide conformations and extends earlier reports

TABLE II

NOE[a] Data on Boc-Cys-Val-Aib-Ala-Leu-Cys-$NHCH_3$

S——————S

$CDCl_3$ at 293 K			10% $(CD_3)_2SO$–$CDCl_3$ at 293 K			$(CD_3)_2SO$ at 318 K		
Resonance Irradiated	NOE Observed	% Enhancement	Resonance Irradiated	NOE Observed	% Enhancement	Resonance Irradiated	NOE Observed	% Enhancement
Val NH	Cys(1) $C^{\alpha}H$	6.3	Aib NH	Val $C^{\alpha}H^{b}$	8.3	Aib NH	Val $C^{\alpha}H$	7.1
Leu NH	Ala NH	2.1	Leu NH	Ala $C^{\alpha}H^{b}$	1.3	$\underline{NH}CH_3$	Cys(6) $C^{\alpha}H$	4.7
	Ala $C^{\alpha}H$	1.5		Ala NH	1.9		$NHCH_3$	2.2
$\underline{NH}CH_3$	Cys(6) $C^{\alpha}H$	6.3		Leu $C^{\alpha}H$	2.3	Val NH	Cys(1) $C^{\alpha}H$	6.6
	$NH\underline{CH_3}$	3.4	Val NH[c]	Cys(1) $C^{\alpha}H$	2.3	Ala NH	Ala $C^{\alpha}H$	4.6
Cys(6) NH	Leu $C^{\alpha}H$	8.1	Cys(6) NH[c]	Leu $C^{\alpha}H$	6.6	Cys(6) NH[d]	Leu $C^{\alpha}H$	5.0
Aib NH	Val $C^{\alpha}H$	8.7	$\underline{NH}CH_3$	Cys(6) $C^{\alpha}H$	6.3			
Ala NH	Leu NH	5.1	Ala NH	Ala $C^{\alpha}H$	2.3			
	Ala $C^{\alpha}H$	5.3	Cys(6) $C^{\alpha}H$	$\underline{NH}CH_3^{c}$	4.6			
Cys(6) $C^{\alpha}H$	$\underline{NH}CH_3$	7.2	Cys(1) $C^{\alpha}H$	Val NH[c]	3.6			
Cys(1) $C^{\alpha}H$	Val NH	4.9	Leu $C^{\alpha}H$	Cys(6) NH[c]	3.2			
Leu $C^{\alpha}H$	Cys(6) NH	6.7	Val $C^{\alpha}H^{b}$	Aib NH	8.3			
Val $C^{\alpha}H$	Aib NH	4.6	Ala $C^{\alpha}H^{b}$	Leu NH	2.6			
Ala $C^{\beta}H_3$	Ala $C^{\alpha}H$	11.8		Ala NH	2.1			
Aib $C^{\beta}H_3$ (highfield)	Aib NH	6.6						
Aib $C^{\beta}H_3$ (lowfield)	Ala NH	11.0						
	Aib NH	1.8						

[a] NOE results are reported for a peptide concentration of ~ 30 m*M*.

[b] Ala and Val $C^{\alpha}H$ resonances are overlapping.

[c] Val, Cys(6), and methylamide NH resonances are overlapping.

[d] Cys(6) and Ala NH resonances are overlapping.

from this laboratory, which illustrated the use of disulfide linkages to stabilize β-[1-4] and γ-turn[48] structures. The extended β-sheet conformation at the Cys residues results in formation of a pair of hydrogen bonds involving the CO and NH groups of the preceding and succeeding residues. Such a structural feature has been noted in cyclic biscystine peptides,[3,18] acyclic cystine derivatives (P. Antony Raj and P. Balaram, unpublished), and in recent studies of an octapeptide analog of somatostatin.[49] Disulfide bridging across a localized antiparallel β-sheet segment may therefore be an important conformational element in disulfide loops where the constraints of cyclization are not dominant.

NOTE ADDED IN PROOF:

The solid state conformation of **1** determined in crystals from dimethylsulfoxide resembles the conformation shown in Fig. 8. However, the Aib-Ala segment adopts a Type II′ β-turn structure (I. L. Karle, personal communication).

This research was supported by a grant from the Department of Science and Technology, Government of India. We thank Dr. T. M. Balasubramanism, Washington State University, St. Louis, for providing the fast atom bombardment mass spectrum.

References

1. Venkatachalapathi, Y. V., Prasad, B. V. V. & Balaram, P. (1982) *Biochemistry* **21**, 5502–5509.
2. Ravi, A., Prasad, B. V. V. & Balaram, P. (1983) *J. Am. Chem. Soc.* **105**, 105–109.
3. Ravi, A. & Balaram, P. (1983) *Biochim. Biophys. Acta* **745**, 301–309.
4. Ravi, A. & Balaram, P. (1984) *Tetrahedron* **40**, 2577–2583.
5. Holmgren, A. (1985) *Ann. Rev. Biochem.* **54**, 237–271.
6. Holmgren, A. (1981) *Curr. Topics Cell. Reg.* **19**, 47–76.
7. Rao, B. N. N., Anil Kumar, Balaram, H., Ravi, A. & Balaram, P. (1983) *J. Am. Chem. Soc.* **105**, 7423–7428.
8. Kishore, R. & Balaram, P. (1984) *J. Chem. Soc. Chem. Commun.* **x**, 778–779.
9. Balaram, P. (1984) *Proc. Ind. Acad. Sci. (Chem. Sci.)* **93**, 703–717.
10. Smith, J. A. & Pease, L. G. (1980) *CRC Crit. Rev. Biochem.* **8**, 315–399.
11. Rose, G. D., Gierasch, L. M. & Smith, J. A. (1985) *Adv. Protein Chem.* **37**, 1–109.
12. Nagaraj, R. & Balaram, P. (1981) *Acc. Chem. Res.* **14**, 356–362.
13. Prasad, B. V. V. & Balaram, P. (1984) *CRC Crit. Rev. Biochem.* **16**, 307–348.
14. Prasad, B. V. V. & Balaram, P. (1982) in *Conformation in Biology*, Srinivasan, R. & Sarma, R. H., Eds., Adenine Press, New York, pp. 133–139.
15. Toniolo, C., Bonora, G. M., Bavoso, A., Benedetti, E., DiBlasio, B., Pavone, V. & Pedone, C. (1983) *Biopolymers* **22**, 205–215.
16. Jones, E. T. & Williams, C. H., Jr. (1975) *J. Biol. Chem.* **250**, 3779–3784.
17. Burleigh, B. D., Jr. & Williams, C. H., Jr. (1972) *J. Biol. Chem.* **247**, 2077–2082.
18. Brown, N. L. (1985) *Trends Biochem. Sci.* **10**, 400–403.
19. Hruby, V. J. (1981) in *Topics in Molecular Pharmacology*, Burgen, A. S. V. & Roberts, G. C. K., Eds., North-Holland Biomedical Press, pp. 99–126.
20. Sarathy, K. P., Krishna, N. R., Lenkinski, R. E., Glickson, J. D., Rockway, T. W., Hruby, V. J. & Walter, R. (1981) *Neurohypophyseal Hormones and Other Biologically Active Peptides*, Schlesinger, D. H., Ed., Elsevier North-Holland, Inc., pp. 211–226.
21. Hruby, V. J., Mosberg, H. I., Fox, J. W. & Tu, A. T. (1982) *J. Biol. Chem.* **257**, 4916–4924.

22. Kishore, R. (1985) Ph.D. thesis, Indian Institute of Science, Bangalore.
23. Iqbal, M. & Balaram, P. (1981) *J. Am. Chem. Soc.* **103**, 5548–5555.
24. Aue, W. P., Bartholdi, E. & Ernst, R. R. (1976) *J. Chem. Phys.* **64**, 2229–2246.
25. Wider, G., Macura, S., Anil Kumar, Ernst, R. R. & Wüthrich, K. (1984) *J. Magn. Reson.* **56**, 207–234.
26. Nagayama, K. & Wüthrich, K. (1981) *Eur. J. Biochem.* **114**, 365–374.
27. Kessler, H. (1982) *Angew. Chem. Int. Ed. Engl.* **21**, 512–523.
28. Balaram, P. (1985) *Proc. Indn. Acad. Sci. (Chem. Sci.)* **95**, 21–38.
29. Wüthrich, K. (1976) *NMR in Biological Research: Peptides and Proteins*, North-Holland, Amsterdam.
30. Stevens, E. S., Sugawara, N., Bonora, G. M. & Toniolo, C. (1980) *J. Am. Chem. Soc.* **102**, 7048–7050.
31. Iqbal, M. & Balaram, P. (1982) *Biopolymers* **21**, 1427–1433.
32. Raj, P. A. & Balaram, P. (1985) *Biopolymers* **24**, 1131–1146.
33. Kishore, R., Anil Kumar, & Balaram, P. (1985) *J. Am. Chem. Soc.* **107**, 8019–8023.
34. Avignon, M., Huong, P. V., Lascombe, J., Marraud, M. & Neel, J. (1969) *Biopolymers* **8**, 69–89.
35. Rao, C. P., Nagaraj, R., Rao, C. N. R. & Balaram, P. (1980) *Biochemistry* **19**, 425–431.
36. Toniolo, C. & Palumbo, M. (1977) *Biopolymers* **16**, 219–224.
37. Inagaki, F., Clayden, N. J., Tamiya, N. & William, R. J. P. (1982) *Eur. J. Biochem.* **123**, 99–104.
38. Pardi, A., Wagner, G. & Wüthrich, K. (1983) *Eur. J. Biochem.* **137**, 445–454.
39. Wagner, G., Pardi, A. & Wüthrich, K. (1983) *J. Am. Chem. Soc.* **105**, 5948–5949.
40. Bystrov, V. F. (1976) *Progr. Nucl. Magn. Reson. Spectrosc.* **10**, 41–48.
41. Glickson, J. D., Gordon, S. L., Pitner, T. P., Agresti, D. G. & Walter, R. (1976) *Biochemistry* **15**, 5721–5729.
42. Bothner-By, A. A. (1979) in *Magnetic Resonance in Biology*, Shulman, R. G., Ed., Academic Press, New York, pp. 177–219.
43. Kartha, G., Bhandary, K. K., Kopple, K. D., Go, A. & Zhu, P. P. (1984) *J. Am. Chem. Soc.* **106**, 3844–3850.
44. Balaram, P., Bothner-By, A. A. & Dadok, J. (1972) *J. Am. Chem. Soc.* **94**, 4015–4016.
45. Wüthrich, K., Billeter, M. & Braun, W. (1984) *J. Mol. Biol.* **180**, 715–740.
46. Shenderovich, M. D., Nikiforovich, G. V. & Chipens, G. I. *J. Magn. Res.* (1984) **59**, 1–12.
47. Aubry, A., Protas, J., Boussard, G. & Marraud, M. (1977) *Acta Crystallogr. Section B* **33**, 2399–2406.
48. Kishore, R. & Balaram, P. (1985) *Biopolymers* **24**, 2041–2043.
49. Wynants, C., Van Binst, G. & Loosli, H. R. (1985) *Int. J. Peptide Protein Res.* **25**, 615–621.

Received August 5, 1986
Accepted November 24, 1986